

Title:

Skeletal Structures for Modeling Complex Chamfers and Fillets

Authors:

Martin Held, held@cs.sbg.ac.at, FB Computerwissenschaften, University of Salzburg, Austria

Peter Palfrader, palfrader@cs.sbg.ac.at, FB Computerwissenschaften, University of Salzburg, Austria

Keywords:

Roof, Chamfer, Fillet, Voronoi diagram, Straight Skeleton

DOI: 10.14733/cadconfP.2018.42-46

Introduction:

A chamfer is a sloping surface or edge that provides a transition between two faces of an object. Similarly, a fillet is the rounding-off of an edge. Both chamfers and fillets may be formed among either inside or outside adjoining faces of an object and are widely applied in manufacturing as well as in other disciplines, e.g., in architecture. Their use ranges from easing otherwise sharp edges to modeling welds and material unremovable by machine tools and ends in purely aesthetic applications.

We use skeletal structures such as the medial axis and its straight-line relative, the straight skeleton, to model both chamfers and fillets. In a nutshell, these skeletal structures partition the plane into regions such that all points of one region are closer to one input entity than to all other input entities. The precise meaning of “closer” and “input entity” depends on the specific skeletal structure. For an input polygon P in the plane \mathbb{R}^2 , both structures can be constructed by wavefront propagation, where an offsetting process causes P to shrink while obeying certain rules. During the offsetting process, an offset structure traces out the interior of P , arriving at each locus with coordinates (x, y) at a specific point in time $t(x, y)$. By interpreting t as z -coordinate one obtains points in \mathbb{R}^3 with coordinates (x, y, t) . The set of all these points forms a three dimensional structure which is commonly called the roof of P .

We extend this standard roof interpretation by a conceptually simple yet powerful method which allows modeling various styles of roofs or sinks. Basically, we still lift the area bounded by P into \mathbb{R}^3 but we generalize how the z -coordinate for each point of the roof-like surface is obtained. We can handle arbitrary polygonal areas with and without holes, and one method also supports boundary curves that consist of circular arcs in addition to straight-line segments.

Voronoi Diagram:

Consider a finite set S of points in the Euclidean plane. The area that is closer to a point $p \in S$ than to any other point of S is called that point's *Voronoi region*, and p is called the defining *site* of that Voronoi region. Each Voronoi region belongs to exactly one site. The boundary of a Voronoi cell is formed by *Voronoi edges*, and the points shared by three or more Voronoi edges are called *Voronoi nodes*. The *Voronoi diagram* is given by the union of the Voronoi edges; see Fig. 1(a) for the Voronoi diagram (clipped to a finite portion of the plane) of a set of 16 point sites. Every Voronoi edge lies on the *bisector* of its two defining sites, i.e., on the set of points equidistant to both sites.

This concept can be illustrated by the prairie-fire analogy: Suppose that fires start in all points of S at the same time, spreading out uniformly in all directions at unit speed. A point in the plane then belongs to the region of the site whose fire reached it first. The loci where two fire waves meet make up the edges of the Voronoi diagram.

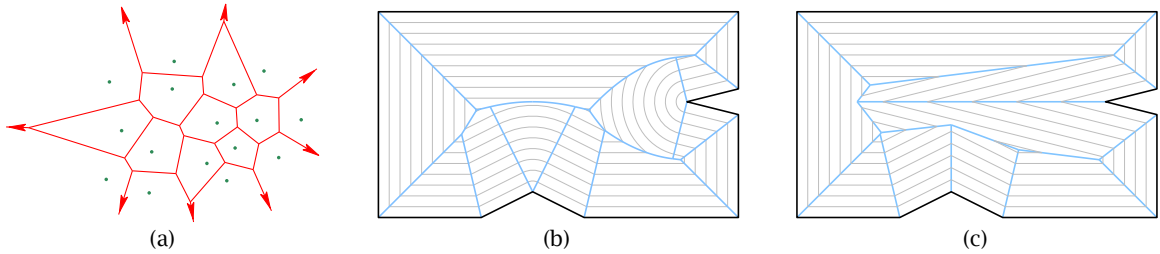


Fig. 1: (a) The Voronoi diagram (red) of 16 point sites (green). (b) The Voronoi-diagram (blue) of an input polygon P (black) with wavefronts (gray) at different times during the propagation process. (c) The straight skeleton (blue) of the same polygon.

The same approach can be used not just for points, but also for more general input sets like a polygon P , with the edges and vertices of P forming the set of sites. Fig. 1(b) shows this propagation at different times together with the resulting Voronoi diagram.

Straight Skeleton:

The straight skeleton of a polygon P was introduced to computational geometry two decades ago by Aichholzer et al. [1] and is defined as the result of a wavefront propagation process similar to that used to illustrate the Voronoi diagram. The main difference is that a reflex vertex v of P does not emanate a circular arc. Instead, the wavefront edges emanated from the edges incident at v move inwards with their common wavefront vertex moving towards the interior of P on their angular bisector. Fig. 1(c) demonstrates this property. As in Voronoi diagrams, the edges of the straight skeleton are the traces of the wavefront vertices, and the straight skeleton tessellates the interior of P into faces with exactly one face per input edge. However, as its name suggests and in contrast to Voronoi diagrams, all its edges are formed by straight-line segments.

Straight skeletons are linked intrinsically with roofs [1]. Regard the edges of a polygon P as the exterior footprint (i.e., bird's eye view) of a building and construct a roof such that water drains to the outside and such that all facets of the roof have the same inclination, with exactly one facet per edge of P . Projecting this unique roof to the two-dimensional xy -plane will result in the straight skeleton of P : The roof facets project to straight skeleton faces, and the ridges and valleys in the roof project to the edges of the straight skeleton.

Generalized Roofs for Modeling Complex Chamfers and Fillets:

In the previous section we mentioned that the straight skeleton of P can be obtained by projecting the unique roof of a building with walls P to the xy -plane. The reverse process, i.e., obtaining the roof from

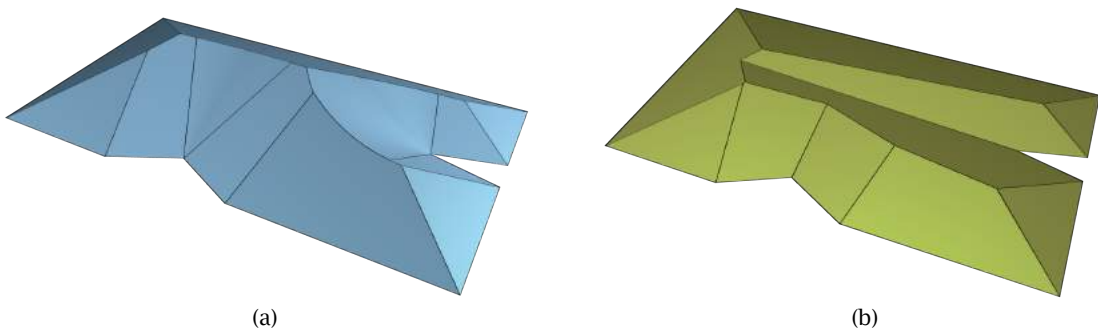


Fig. 2: The roofs induced by the Voronoi diagram (a) and the straight skeleton (b) of the polygon shown in Fig. 1(b) and 1(c).

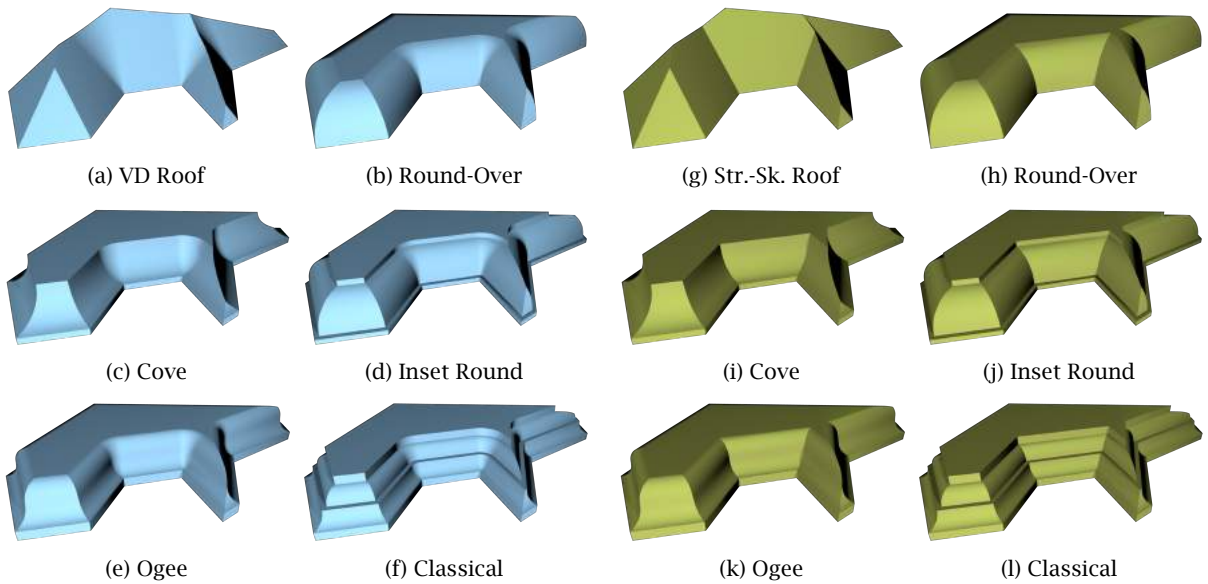


Fig. 3: A sample collection of chamfers based on a Voronoi diagram (left, blue) and mitered chamfers based on a straight skeleton (right, olive-green). (Visit Held’s CGA Lab [3] for larger images and several other examples.)

the straight skeleton, is also possible: Let $\mathcal{W}_P(t)$ be the wavefront of P at time t . Consider all wavefronts over the propagation period and raise each wavefront in the z -coordinate by its time t . This will result in a piecewise-linear and continuous surface $\mathcal{R}(P) := \bigcup_{t \geq 0} (\mathcal{W}_P(t) \times \{t\})$, the roof of P ; see Fig. 2(b). By construction, this surface is a terrain, i.e., every line parallel to the z -axis intersects it in at most one point. The z -isolines of this surface at height t are formed by $\mathcal{W}_P(t) \times \{t\}$.

The same construction principle can also be applied to a wavefront that traced out a Voronoi diagram. Again one gets a continuous surface; see Fig. 2(a). However, such a roof need no longer be piecewise-linear but may contain facets formed by ruled surfaces. As discussed in the previous sections, the actual meaning of the boundary distance t changes in the neighborhood of reflex vertices when basing the construction on a Voronoi diagram rather than on a straight skeleton.

Since there is no stringent theoretical need to use the boundary distance t as z -coordinate for a point on $\mathcal{W}_P(t)$, we can generalize this construction scheme by replacing t by some height function $f: \mathbb{R}_0^+ \rightarrow \mathbb{R}$ of t , which maps every non-negative argument t to a height value. Of course, it is fine to define f only over the interval $[0, t_{max}]$ rather than over all of \mathbb{R}_0^+ if t_{max} is the maximum value of t for which $\mathcal{W}_P(t)$ does not vanish.



Fig. 4: (a) The height function used for obtaining the surfaces shown in Fig. 3(f) and 3(l). The standard height function which results in the roofs of Fig. 3(a) and 3(g) is shown by a dashed line. (b) Mitered chamfers based on a multiplicatively weighted straight skeleton also using the height function from (a).

We use a height function f to generalize the roof $\mathcal{R}(P)$ to a terrain $\mathcal{T}_f(P)$: $\mathcal{T}_f(P) := \bigcup_{t \geq 0} (\mathcal{W}_P(t) \times \{f(t)\})$. For Voronoi-based wavefronts $\mathcal{W}_P(t)$ we can visualize this terrain generated by using $f(t)$ as z -coordinates as follows: Imagine that a solid object is formed by extruding the polygon P along the z -axis. By rotating the height function f around the z -axis we obtain a surface of revolution SR . We now drive an imaginary router bit whose boundary surface matches SR along P such that the tip of the tool follows the boundary of P and such that its axis of rotation stays parallel to the z -axis. Driving that tool along P in the manner described results in a sculpting operation which creates a surface that is identical to the terrain $\mathcal{T}_f(P)$. We note that this interpretation does not hold for mitered wavefronts: The router bit would not be able to machine the valleys that originate at reflex vertices of P .

From a theoretical point of view, the height function f need not be continuous. If, however, the height function is not continuous then the resulting terrain will not be continuous either. Rather, lower and higher portions of the roof will be separated by vertical walls. Similarly, f need not be monotonically increasing. If f is monotonically decreasing then the terrain $\mathcal{T}_f(P)$ does not model a “mountain range” that rises from P but some “underwater landscape”. If f is neither monotonically increasing nor monotonically decreasing then the resulting terrain will contain ditches that wind around peaks like moats used to wind around medieval castles, or rims and ridges that bound areas at lower z -levels, like a crater lake within a volcano.

A collection of sample terrains is shown in Fig. 3. Note that Fig. 3(a) shows the standard Voronoi-diagram induced roof, $\mathcal{R}(P)$, and Fig. 3(g) shows the standard straight-skeleton roof. See Fig. 4(a) for the specific height function used for obtaining the surfaces shown in Fig. 3(f) and 3(l). A chamfering of the outline of an island and chamfers of a polygon with holes are shown in Fig. 5.

If a facet of this terrain is incident to a boundary edge e of P then it constitutes a ruled surface. In particular, all facets of a terrain obtained from a straight skeleton are ruled surfaces. The facet incident at e is defined by sweeping a line such that it passes through one point on its left ridge or valley and through one point on its right ridge/valley. During the entire sweeping process the line stays parallel to e . If the terrain was obtained from a Voronoi diagram then all facets incident at reflex vertices are surfaces of revolution, i.e., portions of the surface SR of the router bit.

Of course, it depends on the mathematical nature of the height function f whether or not it is feasible to model the facets of such a terrain analytically. Most definitely, an exact analytical modeling is possible if f is a piecewise-linear function since then also $\mathcal{T}_f(P)$ is piecewise-linear and, thus, at least in this case it is fairly easy to model the facets of $\mathcal{T}_f(P)$ analytically.

The facets of $\mathcal{T}_f(P)$ can be seen as complex chamfers. For the the standard Voronoi diagram and straight skeleton these chamfers will be symmetric: Locally the two facets on the two sides of a ridge or valley have the same geometry. Asymmetric chamfers can be modeled by resorting to weighted straight skeletons. An additive edge weight causes a facet of $\mathcal{T}_f(P)$ to start at a higher z -level. Multiplicative weights change the “inclination” of a facet by giving it a steep gradient or making it inclined more gently. We refer to [6] for a discussion of the use of additive and multiplicative weights for the generation of roofs and terrains. A sample combination of a multiplicatively weighted straight skeleton with a height function f is shown Fig. 4(b). (The left, front, and right edges of P have multiplicative weights 4, 1, and $1/2$, respectively.)

Implementational Issues:

We have developed a proof-of-concept code to construct complex chamfers (and fillets) based on our terrains. The construction process runs in two stages. In the first stage we use our existing codes VRONI/ARCVRONI [4, 5] and SURFER [7] to generate a Voronoi diagram or a straight skeleton. In our current implementation, conic edges of the Voronoi diagram get sampled and approximated by short straight-line segments. As a result we get a list of polygonal faces, where every face is encoded by a circular list of vertices. Faces in a Voronoi diagram which stem from reflex vertices are triangulated as a triangle fan hinged at the reflex vertex. In addition to the x - and y -coordinates we store with every vertex its appropriate distance t . That is, every vertex can already be seen as a point in three dimensions, and all 2D faces actually form facets of a roof in 3D. In particular, the standard roof $\mathcal{R}(P)$ would be available without further post-processing, cf. Fig. 3(a) and 3(g).

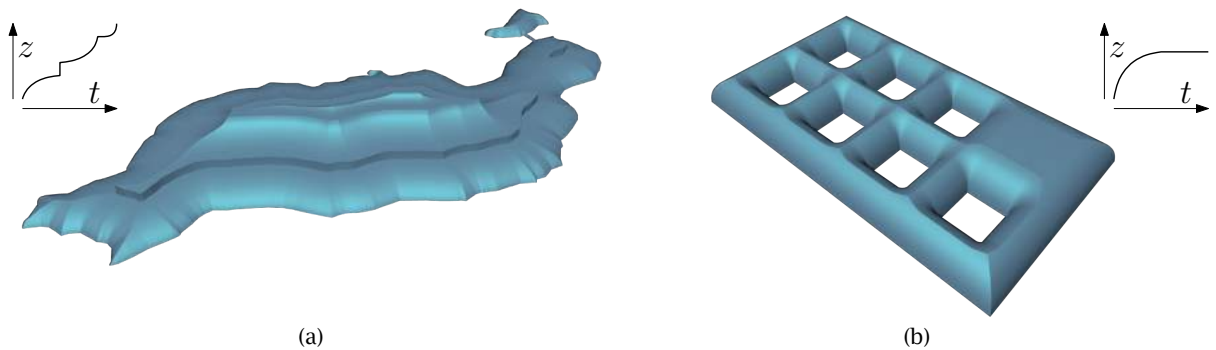


Fig. 5: (a) A Voronoi-based chamfered terrain over the outline of Lanzarote, the easternmost of the Spanish Canary Islands in the Atlantic Ocean. (b) The Voronoi-based chamfered surface of a polygon with square holes using the Round-Over chamfer already seen in Fig. 3(b) and 3(h). The height functions are illustrated in the corners.

In the second step we obtain a terrain by taking a height function and the standard roof from the previous step. Our current implementation supports cubic B-splines as simple yet powerful and flexible height functions. (Recall that repeating one control point p three times forces the cubic B-spline to pass through p , thus creating a sharp corner at p .) Needless to say, our code could be adapted readily to other height functions.

All facets of the standard roof get split into triangles and trapezoids by a set of t -isocontours. These contours correspond to the intersection of horizontal planes with the standard roofs. The isocontours are not spaced uniformly. Rather, the distance between two consecutive contours is chosen in dependence on the gradient of the height function at that time. Finally, the height function is applied to the time component of each vertex, thus obtaining (x, y, z) -coordinates from (x, y, t) -coordinates. For rendering purposes the output of our second stage is imported into Blender [2].

Acknowledgments:

This work was supported by Austrian Science Fund (FWF): P25816-N15 and ORD 53-VO.

References:

- [1] Aichholzer, O.; Aurenhammer, F.; Alberts, D.; Gärtner, B.: A Novel Type of Skeleton for Polygons. *Journal of Universal Computer Science*, 1(12), 1995, 752-761. doi:10.1007/978-3-642-80350-5_65.
- [2] Blender: Free and Open Source Graphics Software. <https://www.blender.org/>.
- [3] Held, M.: Roofs, Terrains, Chamfers and Fillets Based on Skeletal Structures. <https://www.cosy.sbg.ac.at/~held/projects/roofs/roofs.html>.
- [4] Held, M.: VRONI: An Engineering Approach to the Reliable and Efficient Computation of Voronoi Diagrams of Points and Line Segments. *Computational Geometry: Theory and Applications*, 18(2), 2001, 95-123. doi:10.1016/S0925-7721(01)00003-7.
- [5] Held, M.; Huber, S.: Topology-Oriented Incremental Computation of Voronoi Diagrams of Circular Arcs and Straight-Line Segments. *Computer-Aided Design*, 41(5), 2009, 327-338. doi:10.1016/j.cad.2008.08.004.
- [6] Held, M.; Palfrader, P.: Straight Skeletons with Additive and Multiplicative Weights and Their Application to the Algorithmic Generation of Roofs and Terrains. *Computer-Aided Design*, 92, 2017, 33-41. doi:10.1016/j.cad.2017.07.003.
- [7] Palfrader, P.; Held, M.; Huber, S.: On Computing Straight Skeletons by Means of Kinetic Triangulations. *20th Annual European Symposium on Algorithms, Lecture Notes in Computer Science*, volume 7501. Springer-Verlag, 2012, 766-777. doi:10.1007/978-3-642-33090-2_66.